12/2-6-96 JSD

UCRL-ID-122342

Design of a ∅94 cm Mirror Mount for the Petawatt Project on Nova

Ronald "Kip" Hamilton
Gregory L. Tietbohl

October 1995

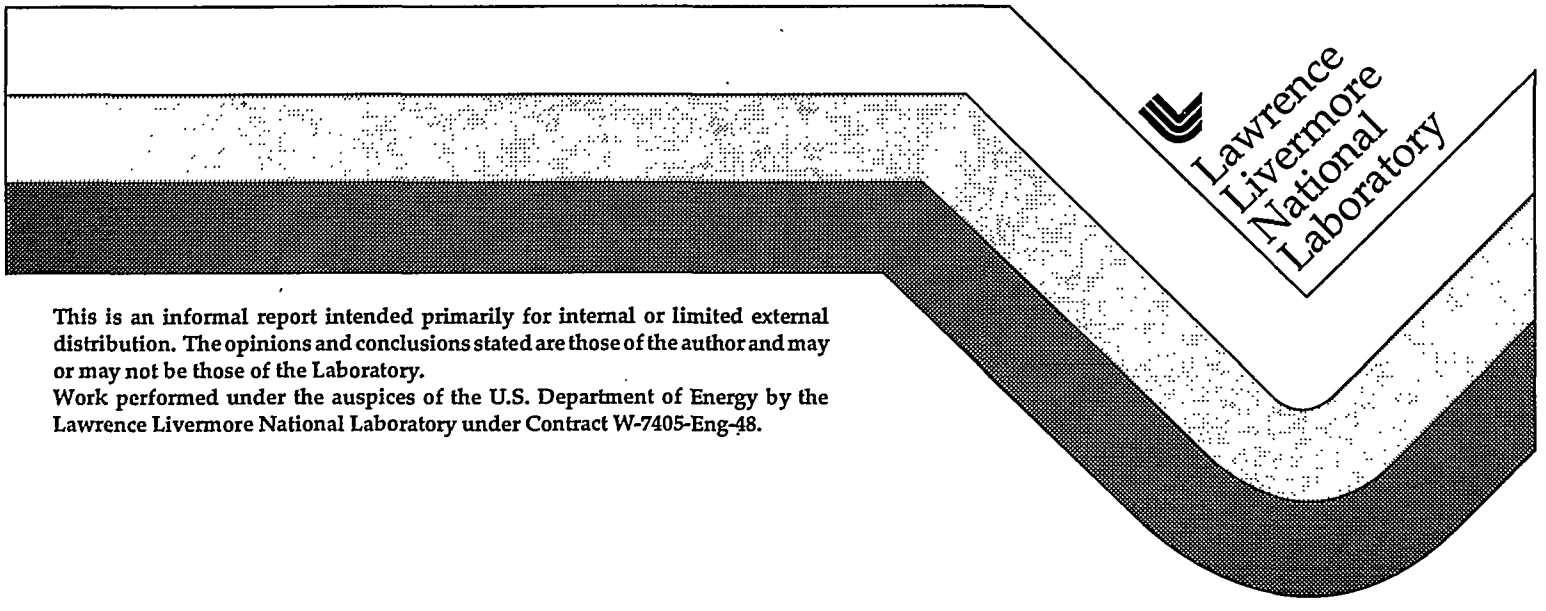

Design of a Ø94 cm Mirror Mount for the Petawatt Project on Nova

Ronald 'Kip' Hamilton
Gregory L. Tietbohl
Lawrence Livermore National Laboratory
Livermore, CA 94550

SUMMARY

We have designed a large optical gimbal mount that will be used on the Petawatt Project currently under construction on the Nova laser. These mounts are designed to hold and tilt Ø94 cm mirrors and gratings that will redirect the Ø60 cm beam through the Petawatt vacuum compressor. Lacking the commercial availability to house this size optic, we have engineered a large mirror mount with a high natural frequency (42 Hz), low self-weight deflection of the mirror (<λ/46), and high positioning accuracy characteristics (<1 μrad using flexures and stepping motors). Analysis details and methodology are presented.

INTRODUCTION

The Petawatt Project, currently under construction within the Nova 10-beam target bay, has a goal to design and construct the world's highest peak power laser.[1] This will be accomplished by rerouting one of Nova's beamlines into a large vacuum vessel where a pulse stretched in time will be temporally compressed prior to entering the Nova 10-beam target chamber. The beam redirection requires five large optical mounts to support turning mirrors and gratings as shown in Figures 1 and 2. These optical mounts are designed for Ø94 cm optics to redirect the Ø60 cm beam through the system.

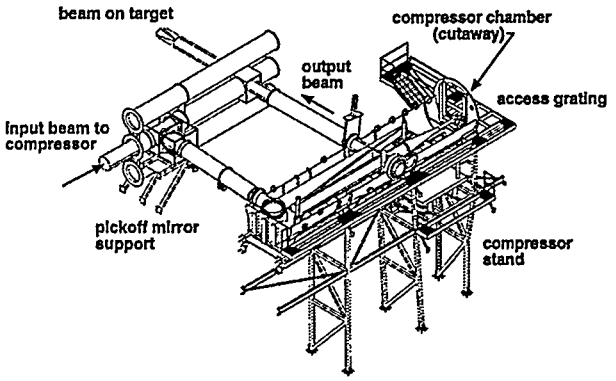

Figure 1 - Computer model of the Petawatt project.

The first of these mounts is for the Ø94 cm pickoff mirror located outside the vacuum chamber. Inside the vacuum compressor chamber are two Ø94 cm mirror mounts and two Ø94 cm grating mounts. To achieve the focus spot size and beam pointing requirements, many variables needed to be carefully considered, including: mirror self-weight distortion, random vibration effects, and alignment resolution requirements.

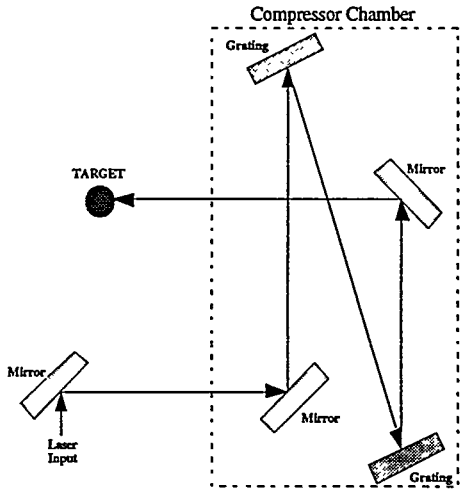

Figure 2 - Petawatt Ø94 cm optic layout.

Design of these mounts requires high stiffness or high fundamental frequency of vibration. Any structure with mass and elasticity will have natural frequencies of vibration, with the lowest frequency being the fundamental. These frequencies of vibration are directly due to ongoing internal exchanges in energy (kinetic to potential and vice versa) within the structure. Natural frequencies of vibration in structures are of a concern if they are close to any external input frequencies. This can cause amplification of motion in the structure or, in the most extreme case, resonance. Should resonance occur, the structure could experience significantly greater deflections and motion than desired. Thus, a high fundamental frequency of vibration of our structure would be advantageous.

The Petawatt optical mounts are located upon other elastic support structures (see Figure 1) which have their own natural frequencies of vibration. Overall system response is therefore dependent on the stiffness of all the components, and the system fundamental frequency of

vibration is always less than that of the most flexible component. A general rule of thumb is to design optical mounts with a fundamental frequency of vibration that is much higher than that of the support structure, which is usually low due to physical limitations. Our experience has shown that fundamental frequencies of large structures are often in the range of 10 to 20 Hz, which suggests that the optical mount should have a fundamental frequency above 50 Hz, for example. Although not the only design criteria, the natural frequency of the mount was a primary concern.

MOUNT SPECIFICATIONS

The mount design will be used to support the following Petawatt optics:

- High Reflection Mirror, 940 mm diameter, 120 mm thick, BK7 substrate.
- Low Leak Mirror, 940 mm diameter, 100 mm thick, BK7 substrate.
- High Reflection Gratings, 940 mm diameter, 120 mm thick, BK7 substrate.

The surface finish of the optics, when mounted, should be less than a tenth-wave for a single pass peak to valley wavefront distortion based on collimated light in reflection at 0.633 μm.

For the mount analysis, the 120 mm thick mirror was used as the worst case due to greatest thickness and highest mass.

DESIGN CONSIDERATIONS

Prior to beginning this analysis, the size and shape of the Petawatt compressor chamber was set, as were the laser beam size, chamber optics, and locations for the optics within the chamber. Therefore the optic mounts had to fit into the available space. Listed below are the major design considerations for the mounts and a brief description of the limitations and/or problems dealt with.

Wavefront Distortion: All of the Petawatt chamber optics are mounted vertically which eliminates out of plane distortion due to gravity. A basic rule of thumb for using radial supports on a large mirror is to locate them on the mirror's center of gravity. All mirrors are sensitive to shifts of these supports away from the center of gravity which can cause unwanted wavefront distortion.

Natural Frequency: Most external vibration sources, (motors, vacuum pumps, etc.), operate at frequencies below 100 hertz (Hz). To prevent laser beam fluctuations caused by these sources, an initial goal of 50 Hz was set as the minimum natural frequency for the mirror mount with the optic installed.

Natural frequency (f) can be defined as:

$$f = \left(\frac{1}{2\pi}\right)\left(\frac{k}{m}\right)^{1/2}$$

where:

k = structural stiffness
m = structural mass

From this equation it can be seen that the natural frequency of a structure increases with stiffness and decreases with increasing mass.

Weight: The compressor chamber was designed with an internal one-ton crane to move the mirror mounts and other items into and around the interior of the vacuum vessel. This limits the weight of the mounts (with optics installed) to less than 2000 pounds. Although this seems generous, the optic alone weighs close to 500 pounds. With an optic this size, the mount requires plenty of additional mass to reach the 50 Hz goal.

Physical Size: The Petawatt compressor chamber has three I-beams welded down its length to support the flooring and mirror mounts as shown in Figure 3.

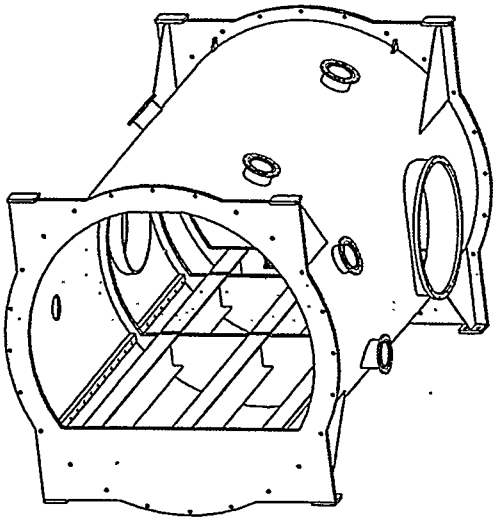

Figure 3 - Isometric view of the center Petawatt vessel.

The tops of these beams are only 28 inches below the tank centerline which is also the laser beam center line. Since the mirror radius is fixed at 18.5 inches, this leaves only 9.5 inches for the mirror mount, translation stages, and flooring.

Physical Shape: The mirrors are oriented to steer the laser beam at least 45° off of normal. With the laser beam profile at 600 mm in diameter, very little mirror mount material can exceed the plane established by the front of the mirror as shown in Figure 4. Any mirror mount material exceeding the front plane would "clip" the laser beam.

The same condition holds for the back of the mirror because a fraction of the beam that leaks though the final turning mirror is needed for beam performance measurements. The sides of the mirror mount are confined by the passing beam lines and interior chamber walls. From the CAD model plan view, it was determined that the entire mirror mount could not exceed a footprint size of 51" x
12".

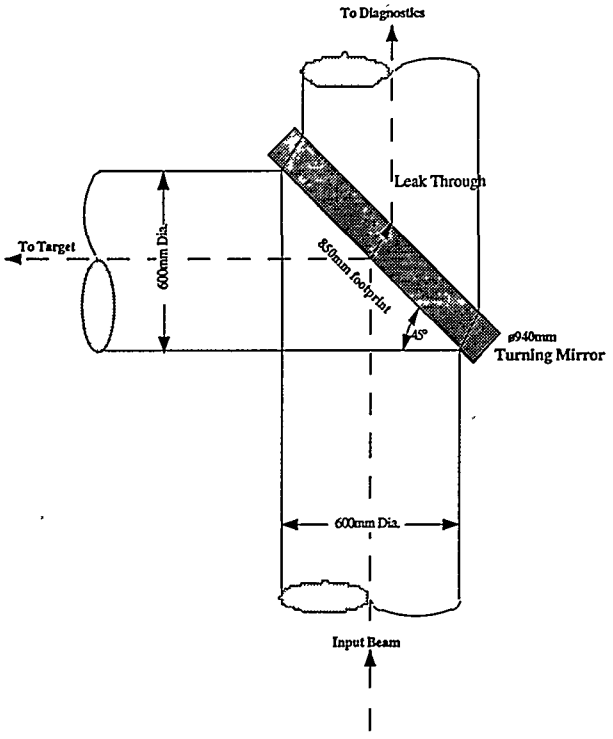

Figure 4 - Sketch of the laser beam on a Petawatt optic.

Material Selection: When selecting a material for a structure to have a high natural frequency it is important that the material used possesses a high specific stiffness (E/ρ). Most common structural materials (aluminum, stainless steel) have the same specific stiffness, including glass. Beryllium as well as some composite materials can have up to six times the specific stiffness of common structural materials but are very expensive or have safety concerns. In order to save money, traditional materials such as stainless steel and aluminum were assumed to be used for construction of the mirror mounts. They are abundant, relatively inexpensive, and have proven reliable in a vacuum environment.

Resolution Specifications: The most stringent resolution specification of any mount is the laser beam pointing requirements of the final turning mirror. The Petawatt mirror mount remote actuators are required to produce <3 μrad of angle at the target source, be vacuum compatible, and are repeatably accurate.

METHODOLOGY

The primary objective of this design process was to analyze the oscillatory motion of the mirror mount, by analyzing each individual mount element in succession, and to increase the component stiffness where possible. The mirror mount was considered a dynamic system and has as many natural frequencies and modes of vibration as degrees of freedom. For this purpose, computer modeling (using COSMOS/M finite element analysis program) was performed to obtain numerical solutions to this multi-degree-of-freedom system.

Our study of the Petawatt mirror mount design began with the optic itself. This produced a baseline fundamental frequency that then changed as additional components were added to the model. The mirror was completely evaluated, such as considering the effects of different mounting schemes and support placements on deformations and fundamental frequency. The inner gimbal ring design was added to the mirror model and the revised system was analyzed for its natural frequency. The process then continued to the outer ring and finally to the mount support frame.

For our mount, a mode of vibration was associated with each natural frequency. Since the equations of motion are coupled, the motion of the masses (optic, inner ring, etc.....) were the combination of the motions of the individual modes.

For each analysis case, the primary modal deformation was examined to determine the appropriate manipulation (of the area moment of inertia of the mass) in order to increase the overall natural frequency of the system.

The following sections list, in detail, the design process and the analytical results to each design step.

GRAVITY EFFECTS

Most commercially available mirror mounts use the typical V-supports. That is, the mirror weight is supported radially by line contact of its rim against two horizontal cylinders located symmetrically in the mount with respect to the vertical centerline.

Our mirror support uses this same concept with a slight variation. Adjustable contoured Teflon pads will be positioned symmetrically about the mount to distribute the load over an area and not line contact.

Using the finite element analysis program, a model of the thick mirror was constructed with the manufacturer's listed mechanical properties for BK7, which include:

- Young's Modulus (E) = 1.19E7 psi
- Poisson's Ratio (u) = 0.207
- Density (r) = 0.0907 lb/in^3

For modeling simplicity, the pad positions were modeled as line contacts. Using only two pads, the gravitational effects on the mirror were analyzed and are shown in Figure 5.

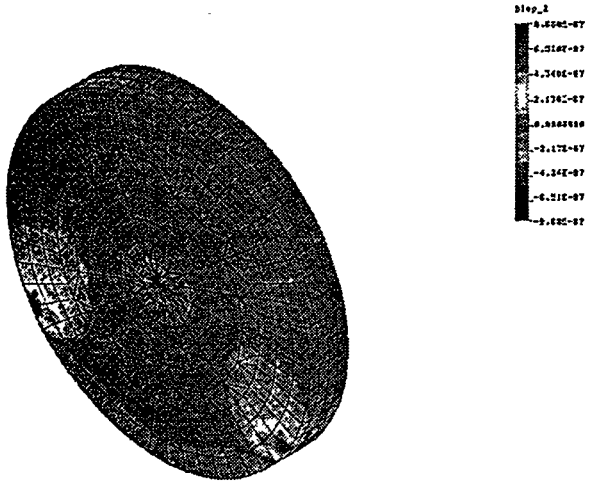

Figure 5 - Wavefront distortion using two pads.

The wavefront distortion of the mirror face from this conservative mounting scheme correlates to a wavefront error of about $\lambda/46$ at 1.053 μm and is considered acceptable.

The actual mount will have the capability to use six contoured pads. For modeling simplicity, it was assumed that each pad would carry a proportional amount of the optic load and were shown as line contacts. This mounting scheme was modeled and is shown if Figure 6.

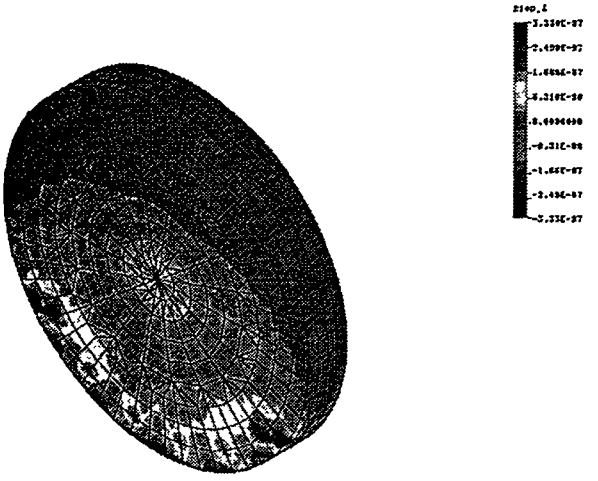

Figure 6 - Wavefront distortion using six pads.

The wavefront distortion of the mirror face from this new mounting scheme correlates to a wavefront error of only $\lambda/124$ at 1.053 μm.

The actual wavefront distortion is estimated to lie somewhere between the two scenarios presented here.

In either case the maximum wavefront distortion occurs at the optics support edges and not directly in the beam footprint. Working radially inward, this distortion rapidly drops off and therefore, the wavefront errors should even be lower than the maximum values listed from the analysis.

MIRROR SUPPORT ANALYSIS

In order to effectively establish a mirror plane, three points of support are required. Common practice suggests that the three points be separated equally about the mirror circumference, at 120° intervals, as incorporated in many commercially available mirror mounts. We verified that this practice produces the highest fundamental frequency of the mirror.

The mirror was modeled as a disk divided into 30° increments. With the left center of the mirror continually held in place with one of the three supports, the other two support positions were rotated equally about the mirror from this fixed support. Each case was then computer analyzed to determine the natural frequency for the support scenario used. Figure 7 shows the case analysis positions used.

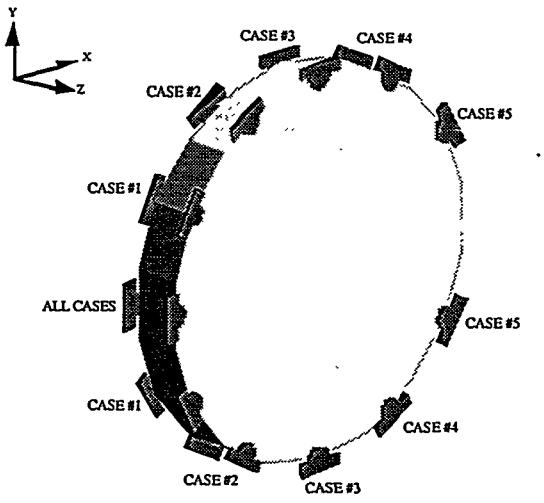

Figure 7 - Petawatt mirror support locations.

Table I shows the natural frequency computational results of the finite element analysis performed on each case scenario. From the table it can be seen that the case of common practice (120° angle increments) is the optimal configuration to use for mirror supports. The Petawatt mirror mount design incorporates this configuration as well.

Case No.	Optic Weight (lbs)	Support Separation Angle (degrees)	Natural Frequency (Hz) Mode Number			
			1	2	3	4
1	460	30	104	308	312	660
2	460	60	158	511	593	839
3	460	90	279	731	836	859
4	460	120	533	576	576	915
5	460	150	367	409	831	946

Table I - Mirror Support Location Results.

MIRROR SUPPORT POSITIONING

With the mirror support positions located 120° apart, we needed to determine their collective orientation with respect to the linear actuator (used to tilt the mirror).

A nominal stainless steel cylinder, used to house the mirror, was modeled to represent the "inner ring" of the gimbal mirror mount design and is shown in Figure 8.

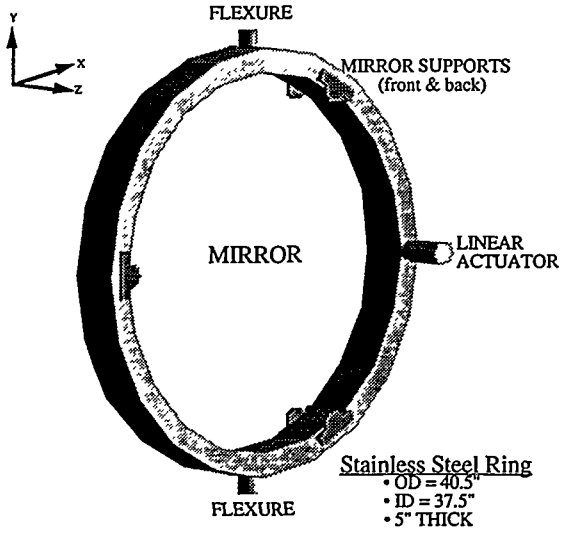

Figure 8 - Model used for support position analysis.

The mirror was modeled with six mirror supports to the ring, three on each mirror surface. The ring was modeled with supports at the top and bottom representing two 1" diameter flexures. The flexures allow rotation of the ring about the y-axis but are fixed in the x, y, and z locations. The linear actuator prohibits the ring from rotation about the flexures thereby totally fixing the ring in space to allow the frequency analysis to be performed.

The three-point support positions were collectively rotated about the z-axis to determine the highest frequency for the mirror at this stage of the design. Figure 9 shows the orientation locations for each case analyzed.

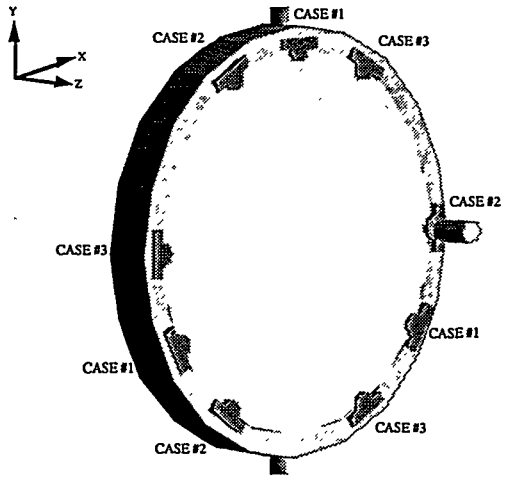

Figure 9 - 120° support orientation locations.

The results of the analysis to properly orient the mirror supports with respect to the actuator are shown in Table II. The orientation that produced the highest natural frequency came from placing a mirror support position directly opposite the optic from the actuator location (Case #3).

Case No.	Optic Weight (lbs)	Support Separation Angle (degrees)	Natural Frequency (Hz) Mode Number			
			1	2	3	4
1	460	120	85	176	198	257
2	460	120	94	98	262	313
3	460	120	98	98	291	313

Table II - Mirror Support Positioning Results.

The drop of the natural frequency from 533 Hz (Table I) to 98 Hz (Table II) was directly due to the addition of the stainless steel ring and its flexibility. The following figure shows the deformation of the ring and mirror (using Case #3) at its lowest natural frequency to illustrate the 98 Hz mode shape. This mode is a flapping of the free side of the ring opposite the linear actuator restraint (like the end of a diving board).

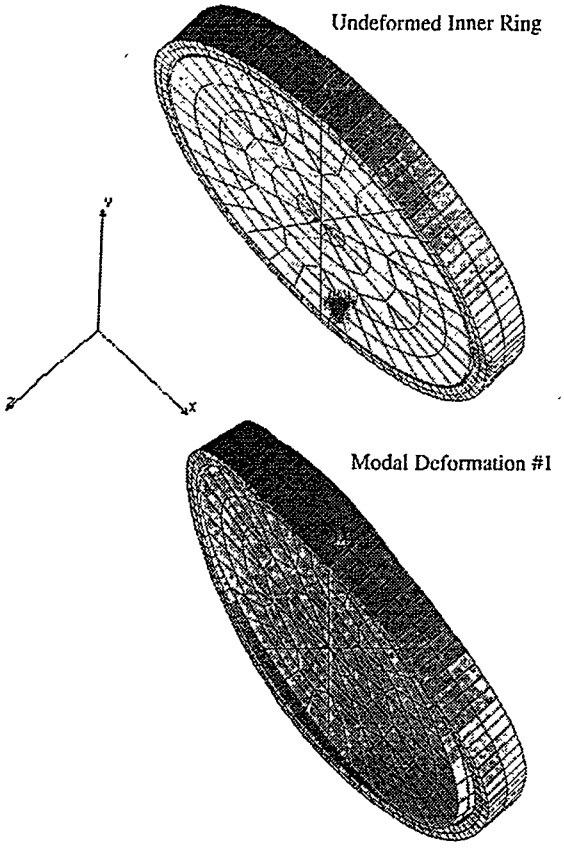

Figure 10 - Modal deformation of Case #3.

Since the first natural frequency produced bending at the free end of the ring, the most obvious method of increasing the natural frequency is to increase the cross-sectional moment of inertia of the ring. The following section addresses this issue in more detail.

INNER GIMBAL RING

With the mirror support locations set, the attention shifted to the design of the inner ring of the gimbal mount. The ring was modeled with the mirror installed and with a flexure at the top and bottom of the ring. These flexures represent the inner ring connection to the outer ring.

Using the finite element analysis program, the mirror was attached to numerous inner ring designs (differing radial cross sections) to determine the highest overall natural frequency of the design to this point.

The following figures are sketches of the inner ring cross sections and their corresponding case number. Each ring houses an optic 5" thick with an 18.5" radius.

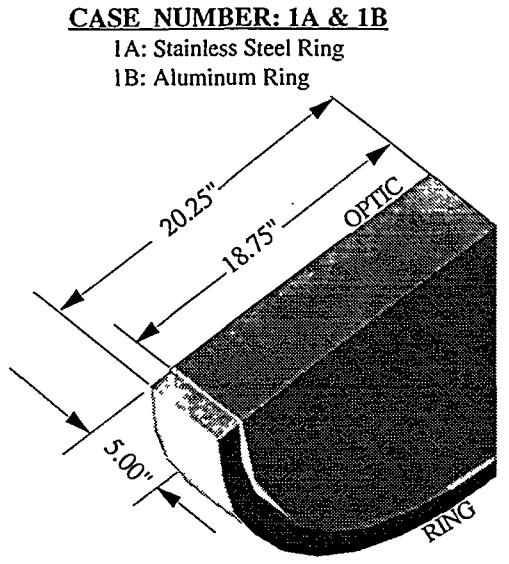

Figure 11 - Case #1 for the inner ring cross section.

Case #1 was identical to our "nominal" ring used in the previous example. Both a stainless steel ring and an aluminum ring were used to determine the frequency effects of the material selection.

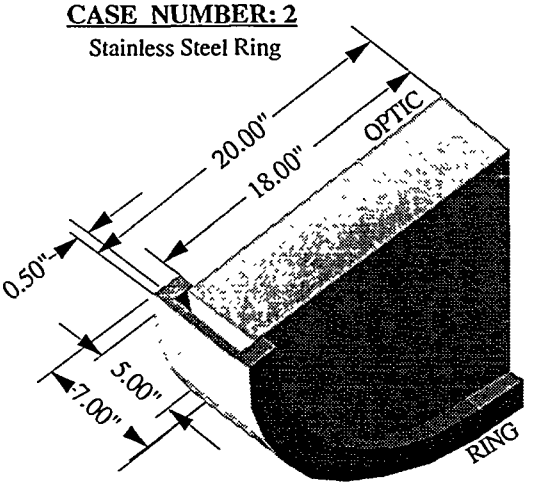

Figure 12 - Case #2 for the inner ring cross section.

Case 2 was a stainless steel ring modeled much like a channel section of steel. Its intent was to increase the cross-sectional moment of inertia in hopes of increasing the natural frequency of the assembly.

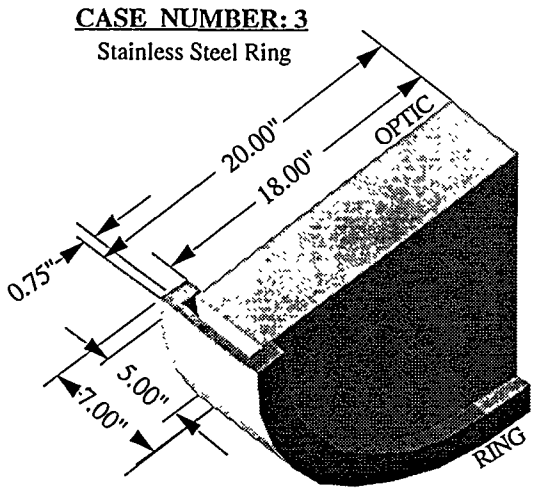

Figure 13 - Case #3 for the inner ring cross section.

Case 3 was modeled like Case 2 except the web was increased by 1/4". It too was modeled to try to increase the ring's cross-sectional inertia.

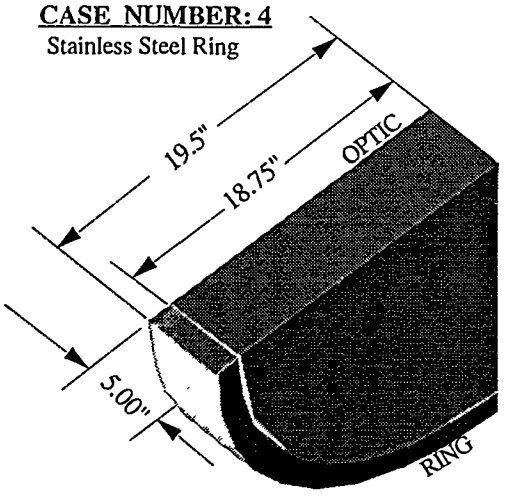

Figure 14 - Case #4 for the inner ring cross section.

Case 4 was an attempt to "thin" the ring from Case 1A to find its natural frequency rate of change.

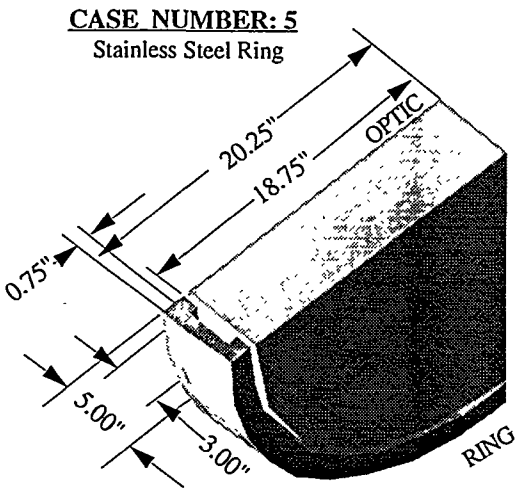

Figure 15 - Case #5 for the inner ring cross section.

Case 5 was chosen to decrease some weight from Case 3 yet maintain the same cross-sectional inertia.

Case 6 was the same as Case 5 but with the additions of aluminum sides to try to increase the cross-sectional inertial of the ring without significantly increasing the overall mass.

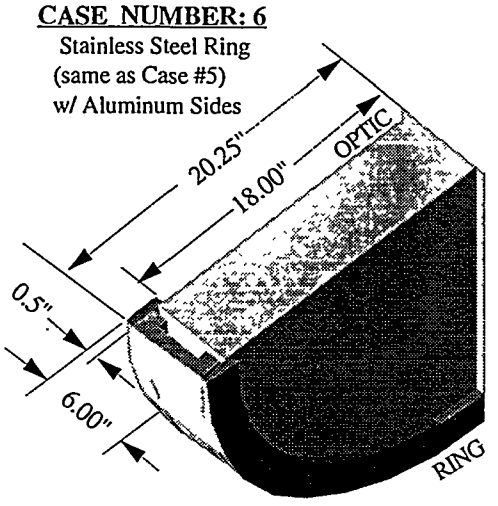

Figure 16 - Case #6 for the inner ring cross section.

The finite element analysis of each of the ring sections was completed and is compiled in Table III. From these results it was determined that the stainless steel ring of Case #1A has the highest fundamental natural frequency.

Case No.	Inner Ring Material	Total Weight (lbs)	Natural Frequency (Hz) Mode Number			
			1	2	3	4
1A	SST	720	89	99	261	311
1B	AL	550	68	76	180	240
2	SST	680	87	110	247	273
3	SST	722	87	113	263	278
4	SST	585	40	68	174	198
5	SST	638	75	79	206	255
6	SST/AL	660	81	91	230	273

Table III - Inner ring frequency results.

Case No.	1A	1B	2	3	4	5	6
Cross Sectional Area (in^2)	7.5	7.5	6.5	7.75	3.75	5.25	7.5
Cross Sectional Inertia (in^4)	15.6	15.6	41.5	44.1	7.81	13.9	31.0

Table IV - Inner ring area and inertia case differences.

For all of the cases presented, the first natural frequency continued to produce bending of the inner ring similar to that shown in Figure 10.

Notice (see Table IV) that Case 1A vs. Case 1B produced significant differences in the natural frequency due to its material selection and not due to the ring inertia. This implies that the inner ring stiffness is too low when made of aluminum.

We assumed that increasing the area moment of inertia of the ring would help but the available space limited the design options for the ring.

In order to continue with the design, the inner ring presented in Case 1A was chosen for use on the Petawatt mirror mount.

OUTER GIMBAL RING

With the optic mounting and inner ring designed, attention shifted to the design of the outer ring of the gimbal mount. The outer ring was modeled with the inner ring attached with flexures at the top and bottom of the outer ring (on the inside diameter). There is also a flexure at each side of the outer ring (on the outside diameter) to represent its attachment points to the mirror support stand. Figure 17 shows a sketch of the ring pair.

Using the finite element analysis program, the mirror and inner ring selections were attached to numerous outer ring designs (differing radial cross sections) to determine the highest overall natural frequency of the ring pair.

The mirror was held constant at 5" thick with a radius of 18.5", and the inner stainless steel ring was held constant at 5" thick with an outside radius of 20.25" and an inside radius of 18.75" (See Case 1A from Section 8).

The outer ring was modeled with supports representing two 1" diameter flexures located at each end. The flexures allow rotation of the outer ring about the x-axis but are fixed in the x, y, and z locations. The linear actuator prohibits the ring from rotation thereby totally fixing the ring pair in space to allow the frequency analysis to be performed.

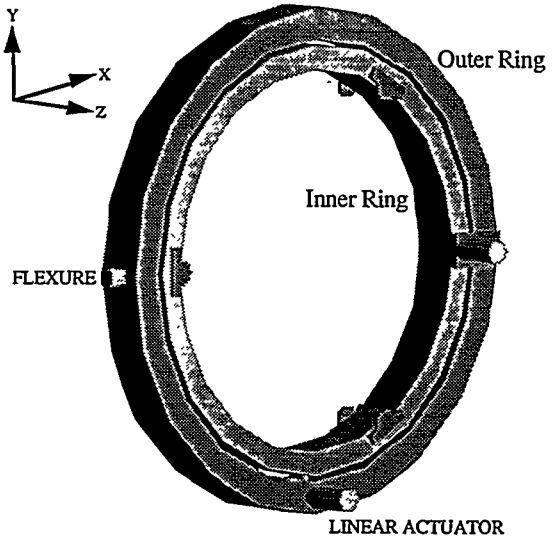

Figure 17 - Part orientation of ring pair.

The following figures show sketches of the cross sections of the ring pair and its corresponding case number.

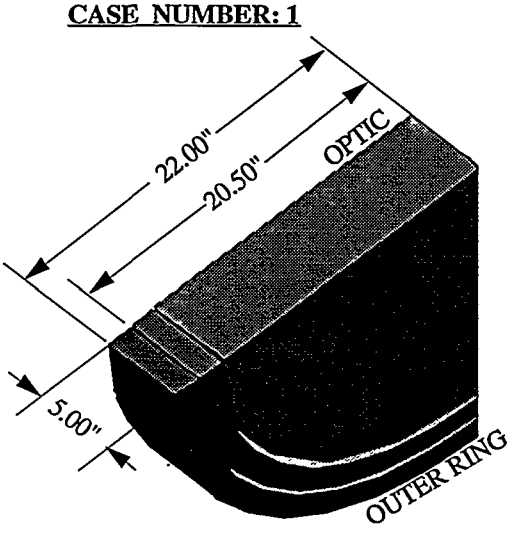

Figure 18 - Case #1 for outer ring analysis.

Case 1 was a baseline because it is simple to fabricate and simple to analyze. Both inner and outer rings have identical cross-sectional dimensions.

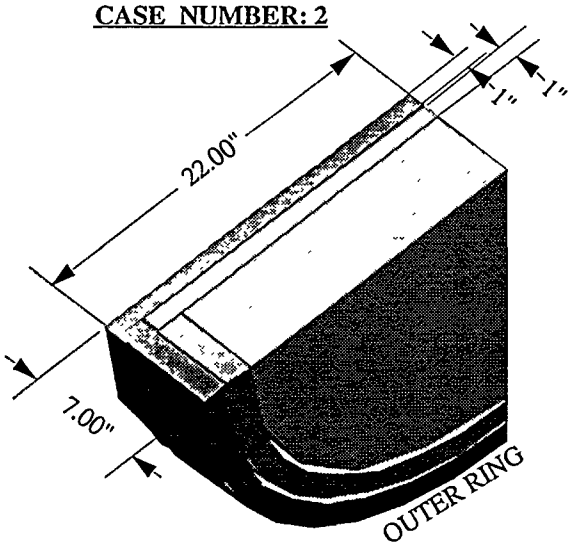

Figure 19 - Case #2 for outer ring analysis.

Case 2 was chosen to show the effects of adding a backing plate onto both rings. Although impractical for our design, it gives one an idea of how to increase the frequency of the ring pair should this come up again.

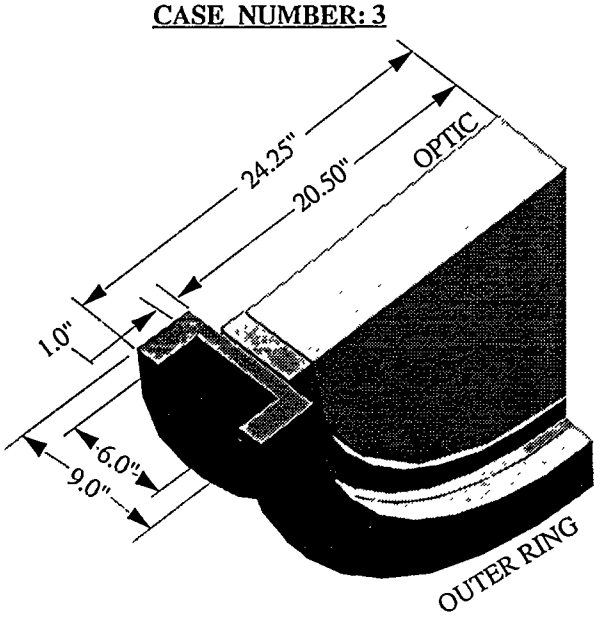

Figure 20 - Case #3 for outer ring analysis.

Case 3 is an attempt to increase the cross-sectional inertia to the maximum space allowed to get an idea of its effect on frequency.

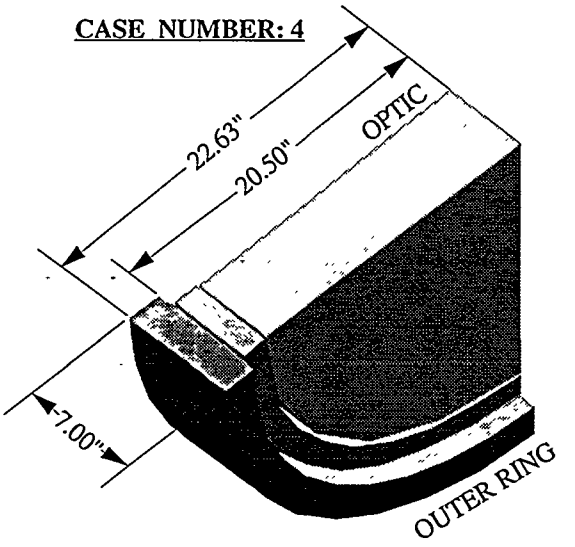

Figure 21 - Case #4 for outer ring analysis.

Case 4 has three subsets to its design:

- Case 4A - Stainless steel inner ring & stainless steel outer ring.
- Case 4B - Aluminum inner ring & stainless steel outer ring.
- Case 4C - Aluminum inner ring & aluminum outer ring.

Case 4 shown is a simple design that is a step above Case 1. This would be easy to fabricate and assembly to the other structural components would be simple.

All of the cases were analyzed with the results presented below in Tables V and VI.

Case No.	Outer Ring Material	Total Weight (lbs)	Frequency (Hz) Mode Number			
1	SST	976	32	57	101	115
2	SST	1880	67	124	157	-
3	SST	1310	35	92	109	148
4A	SST	1323	52	83	119	132
4B	SST	1110	52	73	98	128
4C	AL	765	38	60	93	99

Table V - Outer ring frequency results.

Case No.	1	2	3	4
Cross Sectional Area (in^2)	7.5	31	15.8	14.9
Cross Sectional Inertia (in^4)	15.6	107	160	60.7

Table VI - Outer ring area moment of inertia case differences

Notice that increases in the moment of inertia for the outer ring again produced little or no significant effect on frequency. The lack of space around the mirror also limits the frequency as shown above in Table VI. The backing plate used in Case 2 provides excellent rigidity to the mount and increases its frequency, but its weight is excessive and this design provides no diagnostic leakage.

The fundamental frequency of Case 4A does not change when the inner ring material is changed from stainless steel to aluminum (Case 4B) yet the weight is decreased slightly. The material and fabrication costs can also be decreased using aluminum for the inner ring. An aluminum outer ring (Case 4C) drops the fundamental frequency too far to warrant its use. The outer ring is the "weak" link in the frequency analysis and should be made of stainless steel.

For all of the cases presented, the first natural frequency continued to produce bending of the outer ring similar to Figure 22.

We again assumed that increasing the area moment of inertia of the outer ring would help but the available space limited the design options for the each ring.

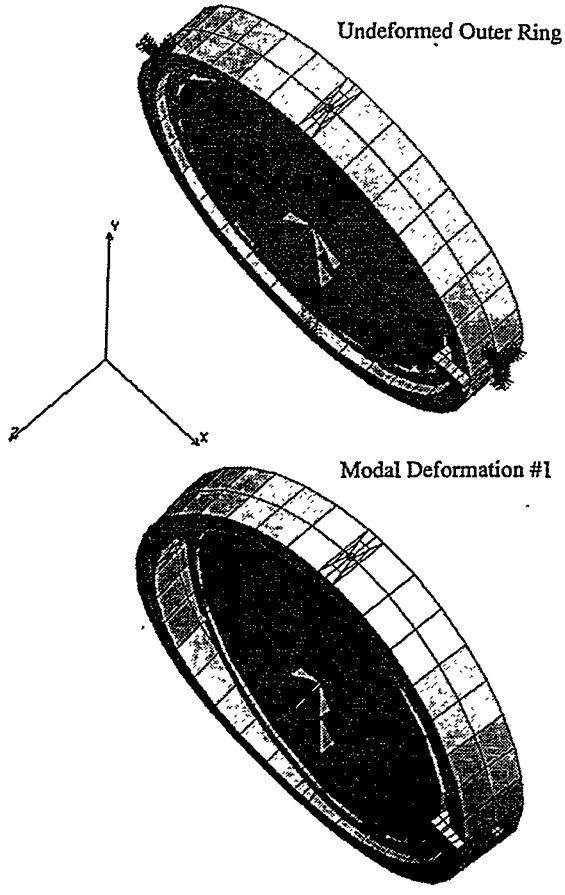

Figure 22 - Outer ring modal deformation.

In order to continue with the design, the ring pair presented in Case 4B was chosen for use on the Petawatt mirror mount. This has a fundamental frequency of 52 Hz.

MOUNT SUPPORT STRUCTURE

Once the design of the gimbal ring pair had been established, the support frame was designed to fit within the maximum footprint mentioned earlier. The entire structure (including mirror) was limited to less than 2000 pounds (crane limit) and could not be intrusive to the beam line at any time.

Using the finite element analysis program, models of the mirror and the ring pair selection (see previous sections) were attached to numerous aluminum support structures to determine the highest overall natural frequency of each design. The finite element model of the sketch shown in Figure 23 was chosen as the best solution (due to all factors involved) and was analyzed with all of the major components attached.

It was assumed the base of the structure was held fixed to represent the attachment of the base to the Petawatt floor. A link between the outer ring and the support was inserted to represent the actuator position of the outer ring as shown in Figure 17.

The entire mirror mount was found to have its lowest natural frequency of 42 Hz as shown in Figure 24. This mode of vibration consists of several motions. The most significant motion belongs to the support structure. The support structure carries the load on two vertical arms, which bend slightly and cause the outer ring to vibrate about the x-axis as shown in Figure 24. The other significant mount motion is an oscillation of the inner ring about the y-axis.

Note that without the mount flexibility (as was the case in the previous section), the fundamental frequency of the ring pair was 52 Hz.

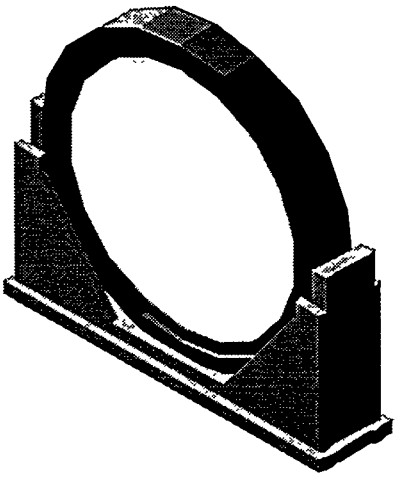

Figure 23 - Sketch of mirror mount design.

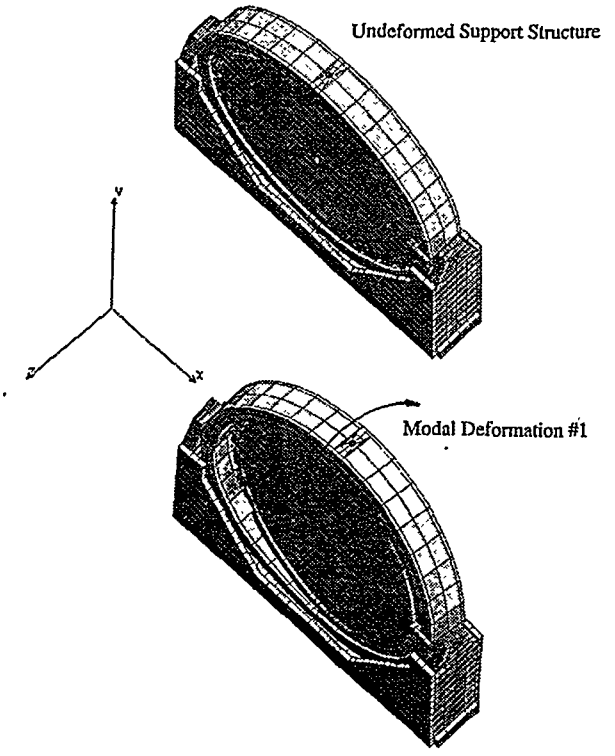

Figure 24 - Support structure modal deformation.

POSITIONING ACCURACY

To achieve the laser beam pointing requirements of the Petawatt system, the final turning mirror mount had to possess remote actuators capable of producing micrometer positioning on target.

DC stepping motors, rated at 200 steps/revolution, were selected to rotate an 80-pitch thread leadscrew. Using micro-stepping capabilities, each microstep results in 0.4μm of linear travel of the leadscrew. With the distance from the final turning mirror to the target set roughly at 14 meters, each microstep of the actuator will produce a 10μm linear offset (<1 μrad angle) on target and is within the project target alignment criteria.

Mirror mount pivot positions often use bearings or bushings to allow mirror tip and tilt. For our positioning requirements, we chose to incorporate flexures in place of those type of pivots. This was done to eliminate stiction and hysteresis often found in bearings and bushings.

At each mirror pivot position, a 1" diameter Lucas Free-flex® flexural pivot was installed. These flexures, shown in a cut-away section in Figure 25, have numerous advantages over conventional pivots by being: stiction free, frictionless, easily installed, predictable, and repeatable.

The combination of the flexures and stepping motors produce the smooth and repeatable high positioning accuracy needed for the Petawatt system.

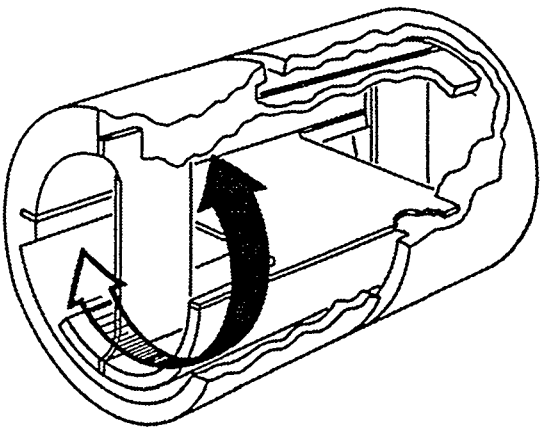

Figure 25 - Cantilevered flexure design.

CONCLUSION

The Petawatt compressor chamber mirror mount proved to be a design challenge due to all the limiting factors involved with the design. The main driver for the design was the natural frequency of the entire mirror mount. Due to weight limits and size constraints, the final frequency value of 42 Hz was achieved.

The design presented here will also be used for mounting the gratings and the final turning mirror, which are thinner than the mirror used in this analysis. In any event, the fundamental natural frequency should only increase above that calculated.

REFERENCES

1. M.D. Perry and G. Mourou, *Science*, 264 917 (1994).

Technical Information Department · Lawrence Livermore National Laboratory
University of California · Livermore, California 94551